HHS Public Access

Author manuscript

Brain Stimul. Author manuscript; available in PMC 2023 May 29.

Published in final edited form as:

Brain Stimul. 2016 ; 9(4): 609–617. doi:10.1016/j.brs.2016.03.014.

Coordinated reset deep brain stimulation of subthalamic nucleus produces long-lasting, dose-dependent motor improvements in the 1- methyl -4- phenyl -1,2,3,6-tetrahydropyridine non-human primate model of parkinsonism

Jing Wang[a], **Shane Nebeck**[b], **Abirami Muralidharan**[c], **Matthew D. Johnson**[d], **Jerrold L. Vitek**[e], **Kenneth B. Baker**[f]

[a]Department of Neurology, University of Minnesota, Minneapolis, MN, USA 55455

[b]Department of Neurology, University of Minnesota, Minneapolis, MN, USA 55455

[c]Department of Neurology, University of Minnesota, Minneapolis, MN, USA 55455

[d]Department of Biomedical Engineering, University of Minnesota, Minneapolis, MN, USA 55455

[e]Department of Neurology, University of Minnesota, Minneapolis, MN, USA 55455

[f]Department of Neuroscience, Cleveland Clinic Lerner College of Medicine, Cleveland, OH, USA 44195

Abstract

Background: Novel deep brain stimulation (DBS) paradigms are being explored in an effort to further optimize therapeutic outcome for patients with Parkinson's disease (PD). One approach, termed 'Coordinated Reset' (CR) DBS, was developed to target pathological oscillatory network activity; with desynchronizing effects and associated therapeutic benefit hypothesized to endure beyond cessation of stimulus delivery.

Objective: To characterize the acute and carry-over effects of low-intensity CR DBS versus traditional DBS (tDBS) in the region of the subthalamic nucleus (STN).

Methods: A within-subjects, block treatment design involving the 1-methyl-4-phenyl-1,2,3,6-tetrahydropyridine (MPTP) non-human primate model of parkinsonism was used. Each treatment block consisted of five days of daily DBS delivery followed by a one week minimum post-treatment observation window. Motor behavior was quantified using a modified rating scale for both animals combined with an objective, upper-extremity reach task in one animal.

Results: Both animals demonstrated significant motor improvements during acute tDBS; however within-session and post-treatment carry-over were limited. Acute motor improvements also were observed in response to low-intensity CR DBS, however both within- and between-session therapeutic carry-over enhanced progressively following each daily treatment. Moreover,

Corresponding Author: Kenneth B. Baker, Department of Neurology, University of Minnesota, 2873H, 2001 6th St SE, Minneapolis, MN 55455, phone: 612-626-8065, fax: 612-626-5685, bakerk6@ccf.org.

Author Contributions:

KBB, JLV and MDJ conceived and designed the experiments. JW, SN, AM, and KBB acquired and analyzed the data. All authors were involved in drafting the article and have approved the final version for submission.

in contrast to tDBS, five consecutive days of CR DBS treatment yielded carry-over benefits that persisted for up to two weeks without additional intervention. Notably, the magnitude and time-course of CR DBS' effects on each animal varied with daily dose-duration, pointing to possible interaction effects involving baseline parkinsonian severity.

Conclusion: Our results support the therapeutic promise of CR DBS for PD, including its potential to induce carryover while reducing both side effect risk and hardware power consumption.

Keywords

Deep Brain Stimulation; Coordinated Reset; MPTP; Neuromodulation; Rhesus Macaque

INTRODUCTION

Deep brain stimulation (DBS) has transformed the treatment of advanced-stage Parkinson's disease (PD), with significant motor benefits attainable when high-frequency, isochronal electrical pulses are delivered chronically to key regions within the basal ganglia thalamocortical (BGTC) 'motor' circuit [1, 2]. Three decades later however, the therapy remains largely unchanged despite advances in our knowledge of the neurophysiological changes that accompany parkinsonian motor signs as well as persistent clinical limitations; including stimulation-induced, therapy-limiting side effects that can be associated with traditional DBS (tDBS) [3–7]. Such considerations have contributed to interest in novel stimulus delivery paradigms that either target directly the putative pathophysiological processes associated with PD, reduce the overall amount of electrical charge delivered to the brain, or both [8–13].

One such approach, termed coordinated reset (CR) DBS, involves the intermittent, pseudo-randomized delivery of brief, low-intensity, spatially-distributed pulse trains for the purpose of desynchronizing 'pathological' neural oscillations [9]. A key advantage of CR relative to tDBS is that its effects are achieved using lower individual pulse amplitudes [9, 14, 15], thereby reducing the risk of provoking side-effects attributable either to the spread of electrical current outside of the target region or to chronic, continuous stimulation of the target itself [7, 16–18]. Furthermore, its desynchronizing effects are hypothesized to endure beyond treatment delivery, such that intermittent therapy may yield benefits that outlast cessation of stimulation by days or weeks [9, 14]. Although the effects of CR DBS currently are well-supported by theoretical models [13, 19–22], in vivo, preclinical or clinical data are limited [14, 15].

Here we used the 1-methyl-4-phenyl-1,2,3,6-tetrahydropyridine (MPTP) non-human primate model of parkinsonism to examine the acute, sub-acute and long-term efficacy profile of CR relative to tDBS. In contrast to the stable, stimulation-dependent motor improvement observed in response to tDBS, the therapeutic profile of low-intensity, CR DBS was marked by progressive, dose-dependent acute and sub-acute changes in motor behavior followed by carry-over effects that endured days after treatment cessation. The overall response profile of CR DBS across individual parkinsonian motor signs was similar to that observed during acute tDBS, further supporting support a potential role for CR in PD DBS therapy.

MATERIALS AND METHODS

Animals and behavioral metrics.

Two adult, female rhesus monkeys (*Macaca mulatta;* Animal *P*, 6kg; Animal *F*, 8kg) were used. Animal care complied with the National Institutes of Health Guide for the Care and Use of Laboratory Animals and all procedures were performed under a protocol approved by the Institutional Animal Care and Use Committee of the University of Minnesota.

Animals were acclimated to the laboratory environment and to passive manipulation of the limbs using positive reinforcement techniques. The severity of the parkinsonian state was indexed using a motor rating scale adapted for use with the parkinsonian non-human primate (mUPDRS) [23]. The mUPDRS is used to rate five key parkinsonian features (rigidity, bradykinesia, akinesia, tremor, and food retrieval [upper-limb only]) on a 4-point scale (0–3; 0 = unimpaired), with ratings derived for both the upper and lower limb (Maximum = 27 points). Scoring was performed during observation of spontaneous behavior and investigator interaction, including passive limb manipulation. Additional objective quantification of upper-limb motor performance was achieved using a cued-reach task in animal *P*, which involved the animal reaching between a start-pad and a computer-generated target displayed on a touch-sensitive screen [24]. A trial initiated when the animal placed its unrestricted hand on a start-pad placed at a fixed, midline location immediately in front of it. After a variable hold period (1.0 – 1.5 sec), the presentation of a circle (8-cm diameter) provided both the target and the go-cue. Successful release of the start pad followed by a touch inside the circular target within specified reaction and reach (3.0 sec) limits triggered a liquid reward. No time limits were imposed for the initiation of consecutive trials.

MPTP Administration.

The MPTP neurotoxin was used to induce a parkinsonian state following standard techniques [25]. For animal *P*, two separate unilateral intracarotid injections (0.6 mg/kg [0.18mg/ml solution], then 0.4 mg/kg [0.12mg/ml solution]; 15-minute infusion) induced a stable, moderate hemiparkinsonian state, with the last injection administered three months prior to the start of treatment. Animal *F* underwent two intracarotid injections of MPTP (0.4 mg/kg; 0.16mg/ml solution; 15-minute infusion) followed by serial intramuscular injections (0.3–0.4 mg/kg, 10mg/ml solution), resulting in a stable, asymmetric parkinsonian state. That animal's final injection occurred two months prior to the first treatment block. Post-operative management for intracarotid procedures included prophylactic antibiotics and opioid analgesics.

DBS Chamber placement.

Pre-operative cranial CT and 7-Tesla MRI were acquired in the anesthetized animal. The merged images were used to plan the placement of cephalic chambers using Cicerone software [26], with the central axis of the chamber positioned and aligned to target the MRI-determined dorsolateral region of the STN. All cephalic hardware, including the chamber and head restraint post, was implanted during an aseptic surgical procedure as detailed previously [25, 27]. Post-surgically, animals were provided ad libitum food and water for a minimum of two weeks with prophylactic pain and infection management provided under

veterinary guidance. For animal *P*, the chamber was oriented 10 degrees lateral to the parasagittal plane and 35 degrees anterior, while for animal *F* the chamber was oriented along the parasagittal plane at an anterior angle of 35 degrees.

STN mapping and DBS lead implantation.

The sensorimotor region of the STN and its borders were mapped using microelectrode recording and stimulation techniques similar to those applied during human functional neurosurgery [28, 29]. A hydraulic microdrive (Narishige Scientific Instruments) was attached to the chamber and used to advance a tungsten microelectrode (impedance 0.5–1.0 MΩ at 1 kHz) into the brain. The acoustically transduced neuronal activity was monitored and qualitative correlations between spontaneous movements or passive manipulation of the limbs used to determine the receptive field characteristics of each isolated neuron. Once the boundaries of sensorimotor STN were determined, a final recording track was performed to establish the target depth for lead placement. Leaving the insertion cannula in place, the microelectrode was removed and replaced with a scaled-down, quadripolar DBS lead consisting of four concentric-ring platinum-iridium contacts [27]. For animal *F*, each ring was 0.63 mm in diameter, 0.50 mm long and separated from one another by 0.50 mm (NuMed Inc., Hopkinton NY). For animal *P*, each ring was 0.86 mm in diameter and 0.50 mm long with an inter-contact spacing of 0.50 mm (St. Jude Medical, Plano TX). Approximately one week later, a post-implant CT was acquired in anesthetized animal and merged with the pre-operative MRI to verify lead location.

The implanted lead was connected to a programmable, implantable pulse generator (IPG) (Brio™, St. Jude Medical, Plano TX), which was placed in a subcutaneous pocket at the level of the chest in animal *P* during a separate surgical procedure [25, 27]. For animal *F*, the IPG was not implanted as the proximal end of the STN DBS lead implanted in that animal was not compatible with the implantable extension cable used with Brio™ IPG. Thus, for this animal the proximal end of the implanted lead was routed to a secondary, dry chamber placed on the cephalic implant and connected to the same model IPG acutely, during each daily stimulation session. In either case, however, the constant-current stimulation was delivered with the animal in the laboratory setting, seated in a standard primate chair with impedance values checked to confirm the integrity of all connections.

Following placement of the DBS lead, each contact was evaluated independently (i.e., pseudo-monopolar stimulation with a distant return) for its effect on parkinsonian motor signs and side-effect profile (e.g., current threshold for muscle contraction). The “optimal” tDBS parameters were operationally defined as those settings (contact and pulse amplitude) that were associated with the greatest improvement in motor signs at the lowest current level, thereafter confirmed to be less than 80% of the current intensity necessary to induce capsular side effects to avoid confounds associated with current spread to the adjacent internal capsule [30] (Figure 1B).

Treatment protocol.

The acute and carry-over effects of traditional and CR DBS were examined using a within-subjects design (Figure 1A). Treatment parameters for each condition are summarized in

Figure 1B. The tDBS parameters were analogous to those applied in PD patients, consisting of continuous, high-frequency (130 Hz) delivery of pulsed (125μs pulse width) electrical charge to a single contact using the metal IPG case (*P*) or the metal head restraint post (*F*) as the anode. The final, therapeutic intensity values for tDBS were 0.55mA (*P*) and 0.5mA (*F*). CR DBS consisted of bursts of stimulus pulses delivered with an individual pulse amplitude approximately one-third that used during tDBS (i.e., 0.2mA for both animals, rounded due to intrinsic 0.05mA resolution of the IPG) in a pseudorandom fashion across the three ventral contacts (cathodes) of the lead using a 3-on: 2-off cycle pattern with the most dorsal contact as the anode (Figure 1C) [14]. Intra- and inter-burst frequencies were set at 150 Hz and 7 Hz, respectively, with pulse width maintained at 125μs.

Each pre-treatment baseline was established by evaluating the animal at least once per day for up to three days before session onset. Thereafter, one of three treatment conditions was examined: tDBS (2 [*P*] or 4 [*F*] hours daily) or CR DBS delivered for either two (CR2) or four (CR4) hours daily. Each block consisted of daily, acute administration of the designated treatment condition over a period of five days followed by a post-treatment observation window to characterize carry-over effects (Figure 1D). During each of the five treatment days, behavior assessments and reach task performance (animal *P* only) measures were collected at a minimum of three time points each day: 1) pre-treatment (DBS-OFF) 2) 30–60 minutes after stimulation onset (DBS-ON) and 3) approximately 90 minutes after cessation of DBS (Figure 1D). During the post-treatment phase, assessments were performed at approximately the same time of day as the initial, DBS-OFF measurement made during the five-day treatment period.

Data Analysis.

Experimental comparisons were designed to characterize changes in motor function at each of four time points relative to DBS administration. *Acute* (i.e., DBS ON) effects were examined using data collected at 30–60 minutes after stimulator activation on each of the five treatment days. The *sub-acute 1* (SA1) time-point was used to examine within-session carry-over and represents data collected 90-minutes after cessation of DBS on each of the five treatment days. *Sub-acute 2* (SA2) data represent the initial, DBS OFF score taken each morning on treatment days 2 – 5 as well as the first assessment made on day 1 of the post-treatment period, thus reflecting carryover effects approximately 19 hours after DBS cessation for each treatment day. Finally, longer term, *post-treatment* carryover was evaluated using data acquired following cessation of treatment.

The effect of each condition on overall motor severity was examined using the total score of the mUPDRS for the hemi-body contralateral to the implanted DBS lead. Task performance for animal *P* was used to characterize treatment-related changes in reaction time (i.e., go-cue presentation to button release), performance accuracy (i.e., ratio of successful touches within the target circle to all touches), and movement velocity of the reach (mm/sec). Statistical analyses were performed using JMP Pro 11 (SAS Institute Inc., Cary, NC USA).

Histology.

Once the experimental endpoint was met, animal *P* was deeply anesthetized with ketamine followed by an overdose of sodium pentobarbital. Thereafter, the animal was perfused transcardially with normal saline (0.9% NaCl) followed by 4% paraformaldehyde with the DBS lead still in place. The brain was blocked in place using a stereotactic frame, post-fixed overnight, and kept in a 15% sucrose solution for 48 hours. 50-μm coronal sections were cut using a freezing microtome and every tenth section (0.5 mm) stained with cresyl violet for DBS lead localization. Tyrosine hydroxylase immunohistochemistry was performed on free-floating sections using an avidin-biotin-peroxidase complex method. Abrupt failure of the cephalic implant and withdrawal of the implanted lead in animal *F* following completion of the final treatment block precluded processing of the tissue for that animal.

RESULTS

Both animals completed each of the three experimental conditions. As illustrated in Figure 1A, the order of treatment blocks for animal *P* was CR2, tDBS, and CR4, whereas the order was CR2, CR4, and tDBS for animal *F*. The entire experimental period for animal *P* spanned a total of 44 days, however due to animal *F*'s participation in an unrelated experimental protocol the delivery of individual treatment blocks was distributed across a period of 243 days. Thus, for animal *F*, the CR2 and CR4 treatment blocks were separated by an off-protocol period of 149 days, while the CR4 and tDBS conditions were separated by 33 days. During the 149 days of off-protocol period, animal F participated in a separate research protocol involving behavioral testing and physiological recordings. Because of the extended time periods between blocks, baseline severity was re-established prior to initiating each experimental condition. As detailed below, each animal experienced a marked (>30%) improvement in motor ratings during acute tDBS, consistent with effect magnitudes reported for PD patients receiving standard, STN DBS therapy [31].

Lead localization and MPTP-induced loss of dopaminergic neurons

The coronal sections presented in Figure 1E depict the effect of the MPTP neurotoxin treatment as well as the position of the DBS lead relative to the STN for animal *P*. TH staining confirmed a marked unilateral reduction in dopaminergic neurons and terminals within the treated relative to the un-treated hemisphere (Figure 1E(i)), while the location of the artifact left by the presence of the DBS lead within the region of the STN is shown in figure 1E(ii) with the area of interest enlarged in figure 1E(iii).

Treatment-related changes in parkinsonian motor signs: mUPDRS

Figure 2 summarizes the development and decay of changes in the DBS-OFF state mUPDRS rating across each treatment blocks by displaying the first rating recorded each morning. Neither animal demonstrated marked, DBS OFF carry-over effects in response to tDBS treatment. Although there is some suggestion of a cumulative effect during the treatment period and carry-over post-treatment for animal *P*, the change is modest (~15%) and well below that observed during acute (i.e., DBS-ON) tDBS (horizontal bar). A similarly modest effect was noted for CR2 DBS in animal *P*. Both animals did, however, demonstrate a clear, step-wise pattern of improvement in response to CR4 DBS during

the treatment period, with a similar pattern appearing in animal *F* in response to CR2. In these cases, therapeutic benefit persisted beyond treatment cessation, with an inverse pattern marked by a progressive decay of benefit over time up to the limits of the post-treatment observation period.

Acute and Sub-acute Effects.—Figure 3 summarizes the change in daily mUPDRS scores for each of the acute, SA1, and SA2 measurement time-points by DBS condition. As shown in the left-hand column, acute tDBS (i.e., DBS ON) was associated with significant improvement in the mean mUPDRS score of 34.0%±7.5% ($\chi^2(1,11)=8.22$, $p<0.005$) and 32.9%±5.7% ($\chi^2(1,16)=10.43$, $p<0.005$) for animal *P* and *F*, respectively. At thirty to sixty minutes after stopping tDBS (SA1) however, those mean changes had diminished to 11.5%±6.0% and 8.9%±3.5% and dropped further thereafter to 7.4%±6.5% and 0.0%±2.8% the next day at the SA2 evaluation for *P* and *F*, respectively. CR4 DBS showed consistent beneficial effects on motor signs for both animals (Figure 3, middle), with significant improvement in the mean mUPDRS scores observed across all three assessments. During acute CR4 stimulation, mUPDRS scores improved an average of 23.6%±4.4% ($\chi^2(1,11)=8.25$, $p<0.005$) and 45.7%±5.4% ($\chi^2(1,16)=10.39$, $p<0.005$), for animal *P* and *F*, respectively. Within-session (SA1) carryover averaged 21.9%±8.4% (*P*: $\chi^2(1,11)=8.22$, $p<0.005$) and 51.4%±2.1% (*F*: $\chi^2(1,10.5)=10.52$, $p<0.005$), while between-session (SA2) scores averaged 23.1%±7.0% (*P*: $\chi^2(1,11)=8.22$, $p<0.005$) and 44.8%±9.9% (*F*: $\chi^2(1,16)=10.39$, $p<0.005$), respectively. In contrast, the effect of CR2 DBS was mixed between animals (Figure 3, right). Whereas minimal changes in mean UPDRS scores were observed across the acute (5.7%±7.3%; $\chi^2(1,11)=4.21$, $p=0.04$)), SA1 (−0.1% ±4.4%; $\chi^2(1,11)=0.007$, n.s.) and SA2 (2.8%±5.6%; $\chi^2(1,11)=1.97$, n.s.)) time points in the moderately affected animal (*P*), animal *F* showed a mean improvement of 81.1% ±8.4% ($\chi^2(1,16)=10.41$, $p<0.005$) in mUPDRS scores acutely, followed by mean SA1 and SA2 improvements of 72.2%±17.1% ($\chi^2(1,16)=10.39$, $p<0.005$) and 41.1%±26.8% ($\chi^2(1,16)=10.38$, $p<0.005$), respectively.

Post-treatment carry-over effects.—The pattern of post-treatment (OFF DBS) carry-over tended to mirror observations made at both the SA1 and SA2 evaluation time points. Accordingly, post-treatment carryover was limited for both animals following the five days of daily tDBS treatment (figure 4, left) as well as for animal *P* in response to CR2 (figure 4, top, right). Persistent carryover effects were, however, observed in both animals in response to CR4 (figure 4, middle) and in response to CR2 in animal *F* (figure 4, bottom, right). Specifically, mean improvements in mUPDRS scores remained significant for animal *P* for up to fifteen days post-treatment, showing a gradual, but consistent decrease in efficacy over that two week period. Meanwhile, mUPDRS ratings for animal *F* remained relatively stable across the first 12 days post-treatment, declining gradually thereafter through day 32, when observations were suspended. Animal *F* also demonstrated significant, post-treatment improvements following CR2, with efficacy decaying but remaining above baseline levels across the nine days of post-treatment observation. Consistent with the lack of sub-acute response already noted, animal *P* did not show a meaningful long-term response to CR2 DBS.

In order to address whether the pattern of therapeutic benefit across individual motor signs was consistent between CR and tDBS, we examined the relative contribution of each mUPDRS sub-scale to overall efficacy. Figure 5 separates the composite mUPDRS percentage change into sub-scale changes, revealing that that the pattern of therapeutic response observed during the CR4 carry-over period (days 1 – 3 post-treatment) is qualitatively similar to what is observed during acute tDBS.

Changes in reach behavior

Figure 6 summarizes changes in peak velocity for animal *P* during the reach phase of the motor task for each of the three DBS conditions. Both tDBS and CR2 DBS show variable acute, DBS ON, changes followed by limited carry-over efficacy. Meanwhile, CR4 DBS was associated with stable performance enhancement both acutely ($F(5,1028)=162.04$, $p<0.0001$) as well as over time during the post-treatment carry-over period ($F(17,1669)=98.28$, $p<0.0001$), largely mirroring the carry-over profile observed in mUPDRS scores (Figure 2). Other features of task performance were unchanged across conditions for both animals, including reaction time and accuracy (data not shown).

DISCUSSION

The present study provides empirical, *in vivo* data supporting the potential of a low-intensity CR DBS approach targeting the STN to produce significant and long-lasting benefit across a range of parkinsonian motor features. Using the MPTP-treated non-human primate model of parkinsonism, we observed a progressive increase in the post-stimulation (i.e., DBS OFF) carry-over effects across the five days of intermittent CR DBS treatment, with those effects outlasting actual stimulus delivery both sub-acutely (between-session) and for up to two weeks following treatment cessation. Our findings are in line with previous theoretical studies [9, 13, 21, 32], observations on the anti-akinetic effects of CR DBS in an MPTP model [14], and its sub-acute effects as reported in a short-term trial in patients with PD [15]. We extend those reports by providing preliminary evidence of a potential dose-response interaction with baseline parkinsonian severity, which is consistent with more recent theoretical postulates concerning a potential relationship between the strength of the underlying pathological coupling [15] and CR-based treatment requirements [33]. However, paradoxical effects of different doses were observed in animal F (Figure 2), which might relate to the variations of the pre-treatment baseline. Furthermore, we provide qualitative evidence that the sub-acute and long-term carry-over effects of CR DBS are not limited to specific motor deficits, but rather improve function across a spectrum of parkinsonian motor signs similar to that observed in response to tDBS.

Although the pathophysiology underlying individual parkinsonian motor signs in PD remains poorly understood, accumulating evidence favors a mechanistic role for changes in the presence and dynamics of frequency-specific, synchronized oscillations across the dopamine-depleted BGTC ‘motor’ circuit [34–38]. Specifically, data from both human PD patients [39] and parkinsonian animal models [40, 41] correlate the emergence and progression (i.e., incidence, strength) of synchronized oscillations in neural activity within specific frequency bands with parkinsonian severity and motor sign manifestation.

Conversely, suppression of some of these same features has been shown to correlate further with therapeutic benefits derived from dopamine-replacement [42] or DBS therapy [43, 44]. Current mechanistic hypotheses concerning tDBS tend to emphasize an active reshaping of neural activity across the BGTC motor circuit by DBS [45, 46], with some suggesting that DBS-induced regularization of firing pattern masks pathological activity, including oscillatory behavior [25, 47].

Coordinated reset DBS was originally designed by Tass [9] to counteract excessive, pathological synchronization across populations of neurons, with potential therapeutic applications in PD as well as other neurological disorders [48, 49]. Its effects are hypothesized to derive from the delivery of spatially- and temporally-distributed electrical pulses across a targeted neural region, putatively disrupting the abnormal synaptic connectivity that may underlie the development and persistence of abnormal neuronal synchrony. To date, in vivo data addressing the therapeutic potential of CR DBS have been limited. It has been shown to increase spontaneous, home-cage activity (i.e., akinesia) in the parkinsonian primate, with post-treatment effects that endured for weeks following treatment cessation [14]. In humans, current data are limited to a single, uncontrolled trial that characterized only its cumulative, sub-acute efficacy profile across three days of treatment [15], with no post-treatment observations reported to address long-term carryover. Of note however, the sub-acute improvements reported by the authors were accompanied by a mean reduction in the averaged peak beta power as recorded from the STN target across all subjects. Unfortunately, long-term clinical studies currently are limited due to the risk of infection associated with prolonged percutaneous externalization of the DBS leads and the lack of an approved, fully-implantable device capable of delivering CR DBS.

Consistent with the findings of the present study, the benefits of tDBS generally depend upon continuous delivery of stimulation [50–52]. Although there is evidence of more enduring anatomical or functional changes associated with tDBS [53–55], the practical impact and clinical significance of such changes are unclear given that individual motor signs begin to recur within seconds to hours of deactivation [50–52, 56, 57]. The side-effects associated with traditional STN DBS also tend to be tightly coupled to stimulus delivery, to the extent that clinical DBS programming typically has the conceptual goal of maximizing coverage of the ‘target’ region(s) while minimizing or avoiding spread of current to adjacent non-motor sub-regions within the target nucleus itself or other structures outside of its borders [3–7, 30, 58–66]. One approach to this problem involves the development of new lead designs (e.g., split-band) that allow for greater ‘sculpting’ of the current fields created during stimulation [67, 68]. Although promising, this tactic fails to consider those side-effects that may be derived in part from constant stimulation of the sensorimotor target region itself [16, 65]; a scenario that may be confounded during bilateral DBS [69, 70]. A CR DBS approach that involves the intermittent delivery of low-intensity pulses may provide comparable motor benefit but be less disruptive to cognitive, affective, and even sensorimotor processing, while reducing power consumption requirements.

In addition to providing preliminary evidence of CR DBS’ ability to improve a range of parkinsonian motor signs, comparable to that achieved during acute (i.e., “ON”) tDBS, data from the current study support a potential interaction between baseline motor severity and

dose parameters. Notably, the time-course and magnitude of the effects of CR DBS varied between animals, most conspicuously in the form of a disparity in the response to CR2 treatment. While four hours of daily CR DBS (CR4) over five days resulted in therapeutic benefit that was either comparable to or exceeded improvements observed during acute (i.e., "ON") tDBS for both animals, CR2 DBS was only effective for the more mildly affected animal. A possible explanation for this disparity may relate to the strength of the underlying coupling [33], such that the shorter treatment duration is simply insufficient for shift the more strongly-coupled ensemble to a desynchronized state. While not conclusive, this finding underscores the importance of further examination of the relationship of CR DBS dose-duration and therapeutic improvement in order to identify the optimal dose-duration.

In conclusion, this study supports the potential superiority of CR DBS as a novel therapeutic alternative to traditional DBS. At the same time, our findings underscore the need for further preclinical and clinical research to characterize fully the carry-over profile, understand its therapeutic mechanisms, and evaluate its relative advantages with respect to mitigating therapy-limiting side-effects currently associated with tDBS. The temporal evolution and devolution of its effects afford a unique opportunity to examine further the relationship between physiological changes across the pallidothalamocortical motor circuit and changes in individual parkinsonian motor features. Future studies may provide insight into the pathophysiology of parkinsonism, the therapeutic mechanisms of CR DBS as a function of individual motor signs, as well as potential physiological markers, or classifiers, that may be of use in the development of algorithms for use in closed-loop DBS systems. Moreover, such studies should address the limitations of the current study, including the limited sample size, the use of non-blinded, qualitative ratings, limited histological verification of lead location, and the interrupted treatment design and restricted carry-over window for animal *F*. Moreover, future studies should examine whether CR DBS is associated with bilateral motor improvements as well as if bilateral treatment is effective. These caveats notwithstanding however, the results provide compelling evidence to support the further exploration of CR DBS for the treatment of PD.

Acknowledgements:

JW was supported by a fellowship award from the Minnesota's Discovery, Research and Innovation Economy (MnDRIVE) program. The work was funded by a research grant from St. Jude Medical. St. Jude Medical was not involved in the collection, analysis, or interpretation of the data and did not play a role in writing the report or in the decision to submit the article for publication. St. Jude medical was afforded an opportunity to review the manuscript prior to submission. We thank Chase Vetruba, Jianyu Zhang, Luke Johnson, and Ben Teplitzky for their technical assistance.

Abbreviations:

mUPDRS	modified Unified Parkinson's Disease Rating Scale
PD	Parkinson's disease
CR	Coordinated reset
DBS	deep brain stimulation
tDBS	traditional deep brain stimulation

STN	subthalamic nucleus
MPTP	1-methyl-4-phenyl-1,2,3,6-tetrahydropyridine
BGTC	Basal ganglia thalamocortical
SA	sub-acute
IPG	implantable pulse generator

REFERENCES

1. Krack P, Batir A, Van Blercom N, et al. Five-year follow-up of bilateral stimulation of the subthalamic nucleus in advanced Parkinson's disease. N Engl J Med 2003; 349: 1925–34. [PubMed: 14614167]
2. Weaver FM, Follett KA, Stern M, et al. Randomized trial of deep brain stimulation for Parkinson disease: thirty-six-month outcomes. Neurology 2012; 79: 55–65. [PubMed: 22722632]
3. Saint-Cyr JA, Trepanier LL, Kumar R, et al. Neuropsychological consequences of chronic bilateral stimulation of the subthalamic nucleus in Parkinson's disease. Brain 2000; 123: 2091–108. [PubMed: 11004126]
4. Dujardin K, Defebvre L, Krystkowiak P, et al. Influence of chronic bilateral stimulation of the subthalamic nucleus on cognitive function in Parkinson's disease. Journal of Neurology 2001; 248: 603–11. [PubMed: 11518003]
5. Rodriguez-Oroz MC, Obeso JA, Lang AE, et al. Bilateral deep brain stimulation in Parkinson's disease: a multicentre study with 4 years follow-up. Brain 2005; 128: 2240–9. [PubMed: 15975946]
6. Deuschl G, Herzog J, Kleiner-Fisman G, et al. Deep brain stimulation: postoperative issues. Mov Disord 2006; 21 Suppl 14: S219–37. [PubMed: 16810719]
7. van Nuenen BF, Esselink RA, Munneke M, et al. Postoperative gait deterioration after bilateral subthalamic nucleus stimulation in Parkinson's disease. Mov Disord 2008; 23: 2404–6. [PubMed: 18951532]
8. Agarwal R and Sarma SV. The effects of DBS patterns on basal ganglia activity and thalamic relay : a computational study. J Comput Neurosci 2012; 33: 151–67. [PubMed: 22237601]
9. Tass PA A model of desynchronizing deep brain stimulation with a demand-controlled coordinated reset of neural subpopulations. Biol Cybern 2003; 89: 81–8. [PubMed: 12905037]
10. Rosin B, Slovik M, Mitelman R, et al. Closed-loop deep brain stimulation is superior in ameliorating parkinsonism. Neuron 2011; 72: 370–84. [PubMed: 22017994]
11. Kuncel AM, Birdno MJ, Swan BD, et al. Tremor reduction and modeled neural activity during cycling thalamic deep brain stimulation. Clin Neurophysiol 2012; 123: 1044–52. [PubMed: 21978653]
12. Wongsarnpigoon A and Grill WM. Energy-efficient waveform shapes for neural stimulation revealed with a genetic algorithm. J Neural Eng 2010; 7: 046009. [PubMed: 20571186]
13. Guo Y and Rubin JE. Multi-site stimulation of subthalamic nucleus diminishes thalamocortical relay errors in a biophysical network model. Neural Netw 2011; 24: 602–16. [PubMed: 21458952]
14. Tass PA, Qin L, Hauptmann C, et al. Coordinated reset has sustained aftereffects in Parkinsonian monkeys. Ann Neurol 2012; 72: 816–20. [PubMed: 23280797]
15. Adamchic I, Hauptmann C, Barnikol UB, et al. Coordinated reset neuromodulation for Parkinson's disease: Proof-of-concept study. Mov Disord 2014.
16. Moreau C, Defebvre L, Destee A, et al. STN-DBS frequency effects on freezing of gait in advanced Parkinson disease. Neurology 2008; 71: 80–4. [PubMed: 18420482]
17. Xie T, Kang UJ, and Warnke P. Effect of stimulation frequency on immediate freezing of gait in newly activated STN DBS in Parkinson's disease. J Neurol Neurosurg Psychiatry 2012; 83: 1015–7. [PubMed: 22696586]
18. Ferraye MU, Debu B, Fraix V, et al. Effects of subthalamic nucleus stimulation and levodopa on freezing of gait in Parkinson disease. Neurology 2008; 70: 1431–7. [PubMed: 18413568]

19. Fan D and Wang Q. Improving desynchronization of parkinsonian neuronal network via triplet-structure coordinated reset stimulation. J Theor Biol 2015; 370C: 157–170.
20. Hauptmann C, Popovych O, and Tass PA. Desynchronizing the abnormally synchronized neural activity in the subthalamic nucleus: a modeling study. Expert Rev Med Devices 2007; 4: 633–50. [PubMed: 17850198]
21. Hauptmann C and Tass PA. Cumulative and after-effects of short and weak coordinated reset stimulation: a modeling study. J Neural Eng 2009; 6: 016004. [PubMed: 19141875]
22. Lucken L, Yanchuk S, Popovych OV, et al. Desynchronization boost by non-uniform coordinated reset stimulation in ensembles of pulse-coupled neurons. Front Comput Neurosci 2013; 7: 63. [PubMed: 23750134]
23. Zhang J, Russo GS, Chen XX, et al. , Deep brain stimulation of monkey globus pallidus externus in experimental parkinsonism, in Soc for Neurosci Abs. 2003.
24. Hendrix C, Agnesi F, Connolly AT, et al. Modulations in Pallidal Local Field Potentials in the Systemic 1-Methyl-4-Phenyl-1,2,3,6-Tetrahydropyridine Nonhuman Primate Model of Parkinson's Disease During a Voluntary Reaching Task. Neural Engineering (NER), 2013 6th International IEEE/EMBS Conference on 2013; 6: 1222–1225.
25. Hashimoto T, Elder CM, Okun MS, et al. Stimulation of the Subthalamic Nucleus Changes the Firing Pattern of Pallidal Neurons. J Neurosci 2003; 23: 1916–1923. [PubMed: 12629196]
26. Miocinovic S, Noecker AM, Maks CB, et al. Cicerone: stereotactic neurophysiological recording and deep brain stimulation electrode placement software system. Acta Neurochir Suppl 2007; 97: 561–7. [PubMed: 17691348]
27. Elder CM, Hashimoto T, Zhang J, et al. Chronic implantation of deep brain stimulation leads in animal models of neurological disorders. J Neurosci Methods 2005; 142: 11–6. [PubMed: 15652612]
28. Baker KB, Boulis NM, Rezai A, et al., Target Selection using Microelectrode Recordings, in Microelectrode Recording in Movement Disorder Surgery, Israel Z and Burchiel K, Editors. 2004, Thieme Medical: New York. p. 138–151.
29. Hutchison WD, Allan RJ, Opitz H, et al. Neurophysiological identification of the subthalamic nucleus in surgery for Parkinson's disease. Ann Neurol 1998; 44: 622–8. [PubMed: 9778260]
30. Xu W, Miocinovic S, Zhang J, et al. Dissociation of motor symptoms during deep brain stimulation of the subthalamic nucleus in the region of the internal capsule. Experimental neurology 2011; 228: 294–7. [PubMed: 20713049]
31. Weaver FM, Stroupe KT, Cao L, et al. Parkinson's disease medication use and costs following deep brain stimulation. Mov Disord 2012; 27: 1398–403. [PubMed: 22975928]
32. Hauptmann C and Tass PA. Restoration of segregated, physiological neuronal connectivity by desynchronizing stimulation. J Neural Eng 2010; 7: 056008. [PubMed: 20811089]
33. Popovych OV, Xenakis MN, and Tass PA. The spacing principle for unlearning abnormal neuronal synchrony. PLoS One 2015; 10: e0117205. [PubMed: 25714553]
34. Hammond C, Bergman H, and Brown P. Pathological synchronization in Parkinson's disease: networks, models and treatments. Trends Neurosci 2007; 30: 357–64. [PubMed: 17532060]
35. Mallet N, Pogosyan A, Sharott A, et al. Disrupted dopamine transmission and the emergence of exaggerated beta oscillations in subthalamic nucleus and cerebral cortex. J Neurosci 2008; 28: 4795–806. [PubMed: 18448656]
36. Brown P, Oliviero A, Mazzone P, et al. Dopamine dependency of oscillations between subthalamic nucleus and pallidum in Parkinson's disease. J Neurosci 2001; 21: 1033–8. [PubMed: 11157088]
37. Nini A, Feingold A, Slovin H, et al. Neurons in the globus pallidus do not show correlated activity in the normal monkey, but phase-locked oscillations appear in the MPTP model of parkinsonism. J. Neurophysiol. 1995; 74: 1800–1805. [PubMed: 8989416]
38. Levy R, Ashby P, Hutchison WD, et al. Dependence of subthalamic nucleus oscillations on movement and dopamine in Parkinson's disease. [see comments.]. Brain 2002; 125: 1196–209. [PubMed: 12023310]
39. Brown P Abnormal oscillatory synchronisation in the motor system leads to impaired movement. Curr Opin Neurobiol 2007; 17: 656–64. [PubMed: 18221864]

40. Bergman H, Wichmann T, Karmon B, et al. The primate subthalamic nucleus. II. Neuronal activity in the MPTP model of parkinsonism. J.Neurophysiol. 1994; 72: 507–520. [PubMed: 7983515]
41. Connolly AT, Jensen AL, Bello EM, et al. Modulations in oscillatory frequency and coupling in globus pallidus with increasing parkinsonian severity. J Neurosci 2015; 35: 6231–40. [PubMed: 25878293]
42. Ray NJ, Jenkinson N, Wang S, et al. Local field potential beta activity in the subthalamic nucleus of patients with Parkinson's disease is associated with improvements in bradykinesia after dopamine and deep brain stimulation. Exp Neurol 2008; 213: 108–13. [PubMed: 18619592]
43. Bronte-Stewart H, Barberini C, Koop MM, et al. The STN beta-band profile in Parkinson's disease is stationary and shows prolonged attenuation after deep brain stimulation. Exp Neurol 2009; 215: 20–8. [PubMed: 18929561]
44. Kuhn AA, Kempf F, Brucke C, et al. High-frequency stimulation of the subthalamic nucleus suppresses oscillatory beta activity in patients with Parkinson's disease in parallel with improvement in motor performance. J Neurosci 2008; 28: 6165–73. [PubMed: 18550758]
45. Bar-Gad I, Elias S, Vaadia E, et al. Complex locking rather than complete cessation of neuronal activity in the globus pallidus of a 1-methyl-4-phenyl-1,2,3,6-tetrahydropyridine-treated primate in response to pallidal microstimulation. J Neurosci 2004; 24: 7410–9. [PubMed: 15317866]
46. Cleary DR, Raslan AM, Rubin JE, et al. Deep brain stimulation entrains local neuronal firing in human globus pallidus internus. J Neurophysiol 2013; 109: 978–87. [PubMed: 23197451]
47. McCairn KW and Turner RS. Deep brain stimulation of the globus pallidus internus in the parkinsonian primate: local entrainment and suppression of low-frequency oscillations. J Neurophysiol 2009; 101: 1941–60. [PubMed: 19164104]
48. Tass PA and Majtanik M. Long-term anti-kindling effects of desynchronizing brain stimulation: a theoretical study. Biol Cybern 2006; 94: 58–66. [PubMed: 16284784]
49. Tass PA and Popovych OV. Unlearning tinnitus-related cerebral synchrony with acoustic coordinated reset stimulation: theoretical concept and modelling. Biol Cybern 2012; 106: 27–36. [PubMed: 22350536]
50. Temperli P, Ghika J, Villemure JG, et al. How do parkinsonian signs return after discontinuation of subthalamic DBS? Neurology 2003; 60: 78–81. [PubMed: 12525722]
51. Cooper SE, Noecker AM, Abboud H, et al. Return of bradykinesia after subthalamic stimulation ceases: relationship to electrode location. Exp Neurol 2011; 231: 207–13. [PubMed: 21736878]
52. Cooper SE, McIntyre CC, Fernandez HH, et al. Association of deep brain stimulation washout effects with Parkinson disease duration. JAMA Neurol 2013; 70: 95–9. [PubMed: 23070397]
53. Akita H, Honda Y, Ogata M, et al. Activation of the NMDA receptor involved in the alleviating after-effect of repeated stimulation of the subthalamic nucleus on motor deficits in hemiparkinsonian rats. Brain Res 2010; 1306: 159–67. [PubMed: 19766606]
54. Khaindrava V, Salin P, Melon C, et al. High frequency stimulation of the subthalamic nucleus impacts adult neurogenesis in a rat model of Parkinson's disease. Neurobiol Dis 2011; 42: 284–91. [PubMed: 21296669]
55. Shen KZ, Zhu ZT, Munhall A, et al. Synaptic plasticity in rat subthalamic nucleus induced by high-frequency stimulation. Synapse 2003; 50: 314–9. [PubMed: 14556236]
56. Hristova A, Lyons K, Troster AI, et al. Effect and time course of deep brain stimulation of the globus pallidus and subthalamus on motor features of Parkinson's disease. Clin Neuropharmacol 2000; 23: 208–11. [PubMed: 11020125]
57. Vitek JL, Hashimoto T, Peoples J, et al. Acute stimulation in the external segment of the globus pallidus improves parkinsonian motor signs. Mov Disord 2004; 19: 907–15. [PubMed: 15300655]
58. Pinsker M, Amtage F, Berger M, et al. Psychiatric side-effects of bilateral deep brain stimulation for movement disorders. Acta Neurochir Suppl 2013; 117: 47–51. [PubMed: 23652656]
59. Mikos A, Bowers D, Noecker AM, et al. Patient-specific analysis of the relationship between the volume of tissue activated during DBS and verbal fluency. Neuroimage 2011; 54 Suppl 1: S238–46. [PubMed: 20362061]
60. Schroeder U, Kuehler A, Lange KW, et al. Subthalamic nucleus stimulation affects a frontotemporal network: a PET study. Annals of neurology 2003; 54: 445–50. [PubMed: 14520655]

61. Hershey T, Wu J, Weaver PM, et al. Unilateral vs. bilateral STN DBS effects on working memory and motor function in Parkinson disease. Exp Neurol 2008; 210: 402–408. [PubMed: 18162183]

62. McIntyre CC, Richardson SJ, Frankemolle AM, et al. Improving postural stability via computational modeling approach to deep brain stimulation programming. Conf Proc IEEE Eng Med Biol Soc 2011; 2011: 675–6.

63. Tommasi G, Krack P, Fraix V, et al. Effects of varying subthalamic nucleus stimulation on apraxia of lid opening in Parkinson's disease. J Neurol 2012; 259: 1944–50. [PubMed: 22349870]

64. Homer MA, Rubin SS, Horowitz TD, et al. Linguistic testing during ON/OFF states of electrical stimulation in the associative portion of the subthalamic nucleus. Neuromodulation 2012; 15: 238–45; discussion 245. [PubMed: 22672051]

65. Jahanshahi M, Obeso I, Baunez C, et al. Parkinson's disease, the subthalamic nucleus, inhibition, and impulsivity. Mov Disord 2015; 30: 128–40. [PubMed: 25297382]

66. Tagliati M, Barnaure I, Martin C, et al., Long-Term Gait Deterioration after Bilateral STN DBS is not due to the Natural Progression of Parkinson's Disease., in American Academy of Neurology. 2008; Chicago, IL.

67. Martens HC, Toader E, Decre MM, et al. Spatial steering of deep brain stimulation volumes using a novel lead design. Clinical neurophysiology : official journal of the International Federation of Clinical Neurophysiology 2011; 122: 558–66. [PubMed: 20729143]

68. van Dijk KJ, Verhagen R, Chaturvedi A, et al. A novel lead design enables selective deep brain stimulation of neural populations in the subthalamic region. J Neural Eng 2015; 12: 046003. [PubMed: 26020096]

69. Alberts JL, Hass CJ, Vitek JL, et al. Are two leads always better than one: an emerging case for unilateral subthalamic deep brain stimulation in Parkinson's disease. Exp Neurol 2008; 214: 1–5. [PubMed: 18718469]

70. Alberts JL, Voelcker-Rehage C, Hallahan K, et al. Bilateral subthalamic stimulation impairs cognitive-motor performance in Parkinson's disease patients. Brain 2008; 131: 3348–60. [PubMed: 18842609]

A.

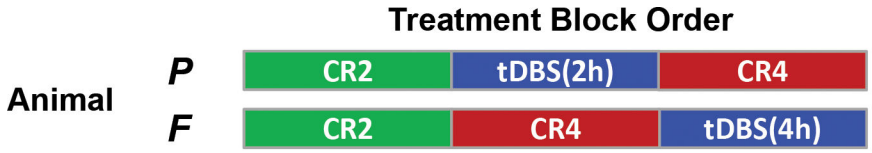

B.

PARAMETERS	tDBS	CR DBS
Intensity (mA)	0.55(*P*); 0.5(*F*)	0.2
Pulse width (μs)	125	125
Frequency (Hz)	130	Interburst: 7 Intraburst: 150
Pulses per burst	*n.a.*	5
Pulse cycling (*m:n*)	*n.a.*	3:2

C.

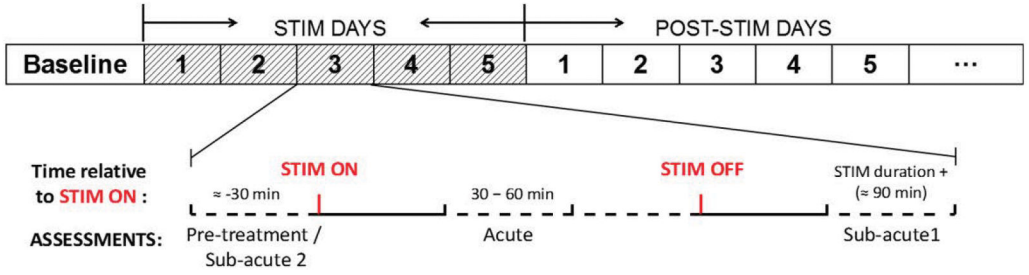

D.

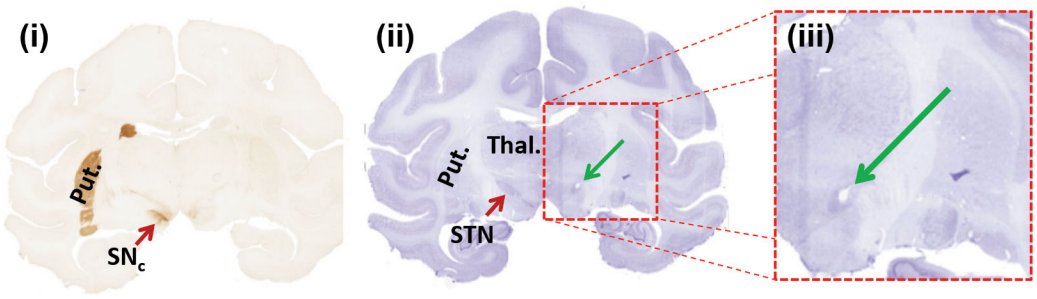

Figure 1.

(A) The order of the individual DBS treatment blocks as applied to each animal over the course of the study. **(B)** Stimulation parameters used for each treatment condition. With the exception of the duration of stimulus delivery (i.e., 2- versus 4-hours), the same stimulation parameters were applied during both the CR2 and the CR4 conditions. **(C)** Schematic illustration of the pattern of pulses used during CR DBS (modified from supplementary figure 1 in [14]). **(D)** Schematic overview of the sub-stages within each treatment block. As illustrated, a pre-treatment baseline period was followed by five days of daily stimulation (Treatment Phase) followed by a post-treatment phase designed to examine the magnitude

and duration of carry-over effects. The magnified inset depicts the daily data collection timeline for a treatment phase day. **(E)** Coronal sections from animal *P* illustrating (**i**) the loss of TH+ neurons in the MPTP-treated hemisphere (right) and the relative location of the artifact (green arrow) left by placement of the DBS lead in the STN (**ii & iii**).

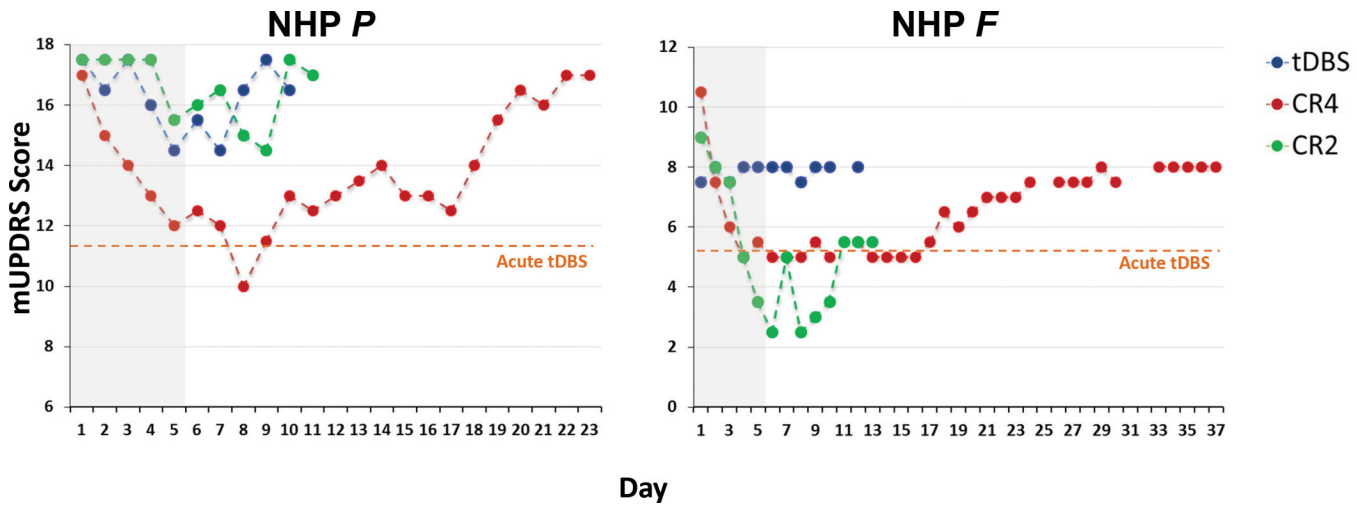

Figure 2.

The initial, composite mUPDRS rating recorded at the beginning of each daily session across the experimental period for animal *P* (left) and animal *F* (right). Each point represents the OFF DBS rating recorded each morning, including that taken just prior to stimulation delivery during each five-day treatment phase (shaded gray region). Data are color-coded to represent the type of stimulation delivered across the five-day treatment block. As noted in the text, follow-up and continuity for animal F was disrupted due to its on-going participation in an unrelated experimental protocol. The dashed, gold line represents the mUPDRS score for each animal during acute (i.e., DBS ON) tDBS.

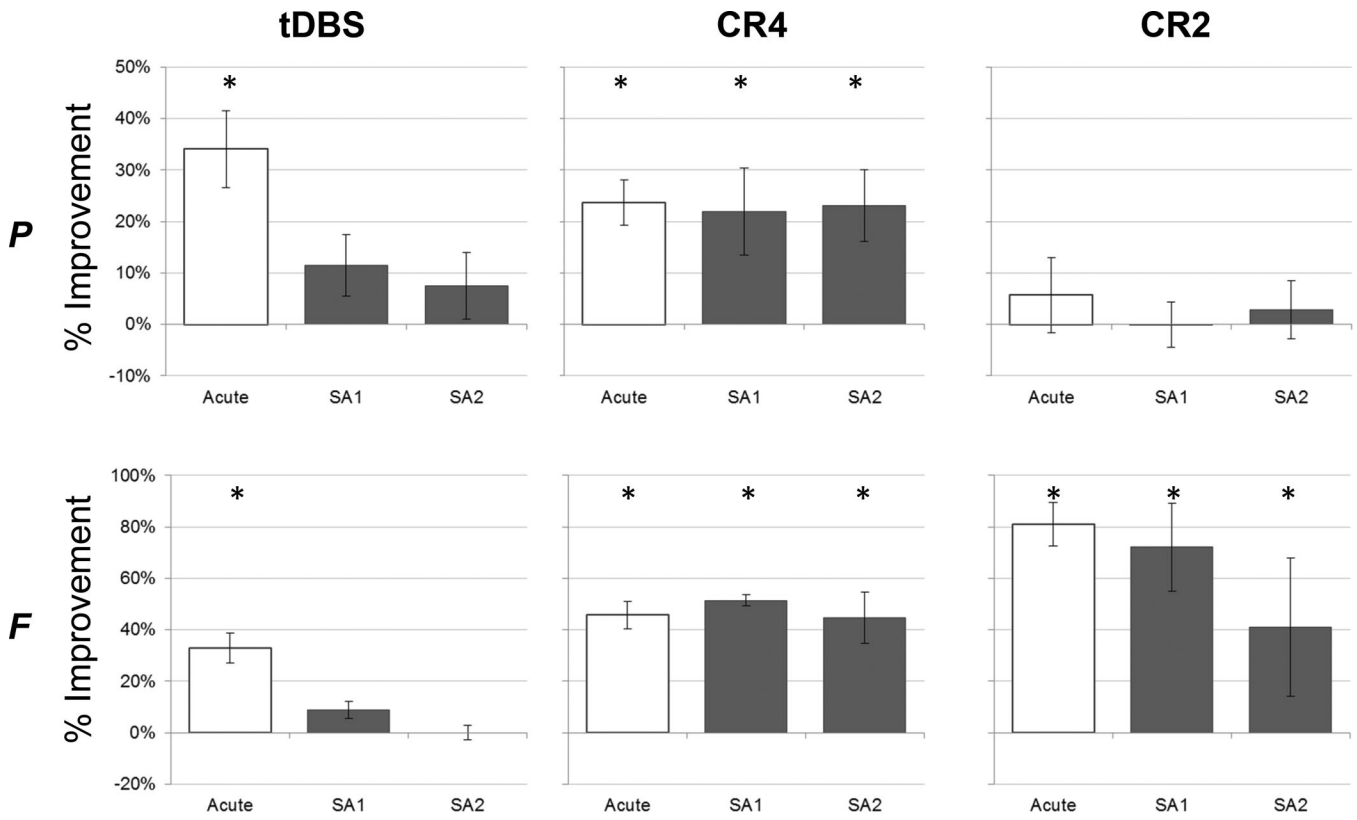

Figure 3.

The mean (+/− SD) acute and sub-acute (SA1 & SA2) change (%) in mUPDRS scores for each animal and treatment condition across the five treatment days. * Significantly different from baseline ($p < 0.05$)

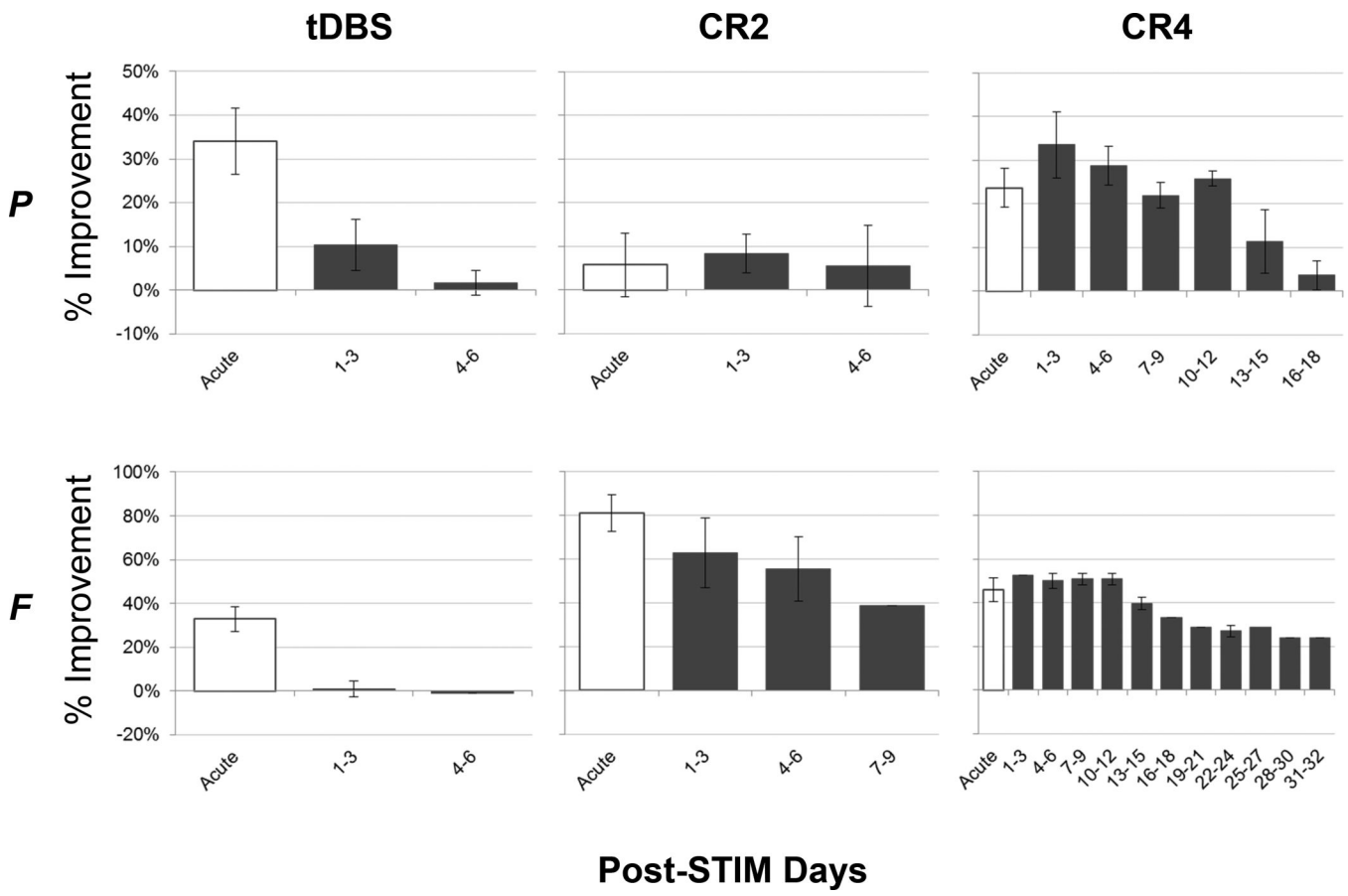

Figure 4.

Post-treatment carry-over varied by treatment condition and animal. The mean (+/− SD) changes (%) in mUPDRS scores for each animal as a function of treatment condition following cessation of DBS (post-treatment carry-over). The acute data (white bars) are the same as shown in figure 2 and reproduced here for reference. During the post-treatment period, data are averaged using non-overlapping, three-day windows.

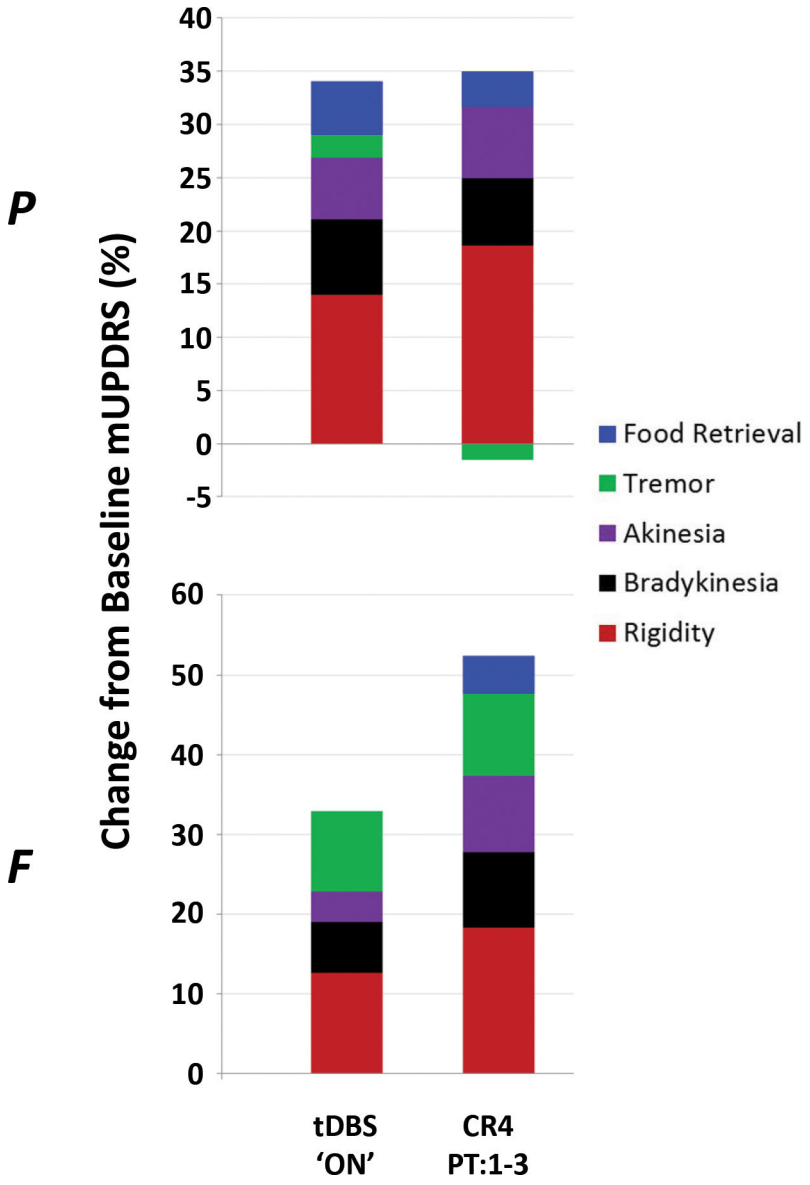

Figure 5.

A comparison of the treatment-related changes in mUPDRS during acute (i.e., ON) tDBS and the average change observed across days 1 – 3 post-treatment following the CR4 DBS condition. Here, the composite score is further broken down to reveal the individual changes observed across the five major subscale categories of the scale.

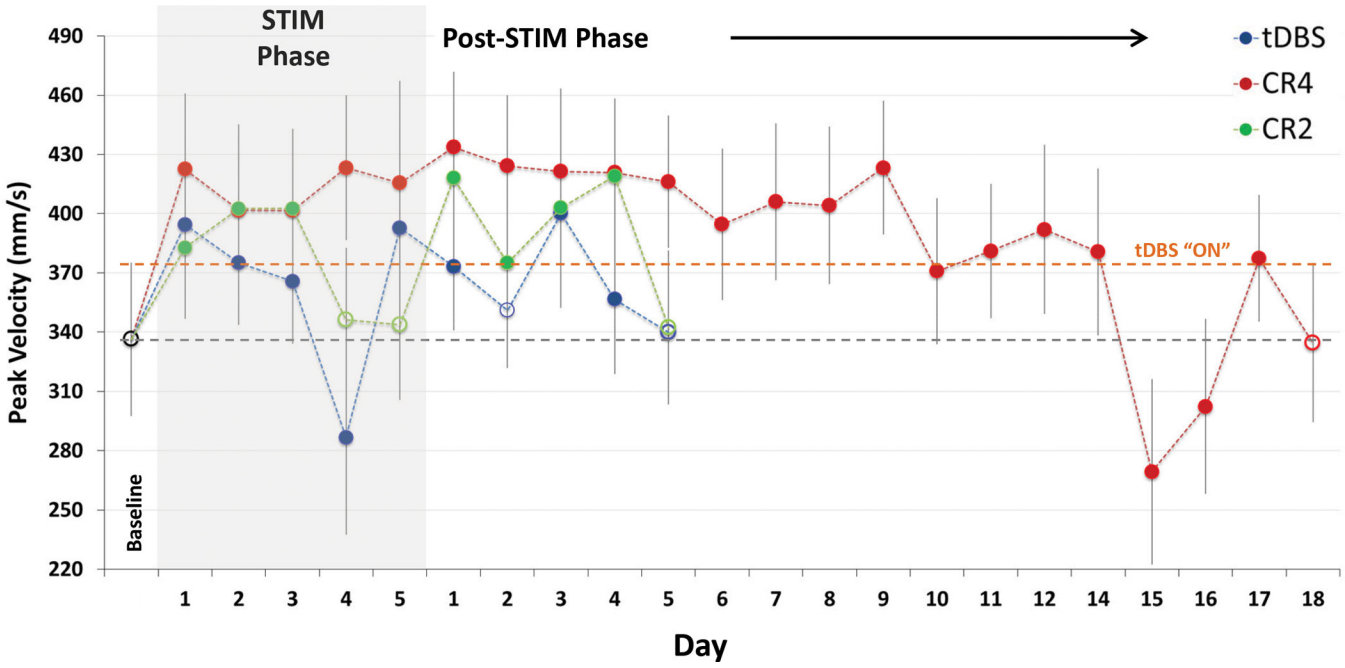

Figure 6.

Peak wrist velocity during the reach / reward task in NHP *P* for traditional, acute CR DBS and post-CR DBS carry-over relative to baseline (far left) performance. An average increase of 23% was observed during acute CR4 DBS, with significant ($p < 0.01$, Dunn's method) carry-over for 14 days after cessation of treatment (Filled circles represent significant difference from baseline performance). The rebound effect on day 15 also was significant and warrants further investigation.